Dynamics character of swirling flame investigated by OH and CH2O planar laser-induced fluorescence

Yan, Hao, Zhang, Shaohua, Yu, Xilong

Hao Yan, Shaohua Zhang, Xilong Yu, "Dynamics character of swirling flame investigated by OH and CH2O planar laser-induced fluorescence," Proc. SPIE 11046, Fifth International Symposium on Laser Interaction with Matter, 110460Q (29 March 2019); doi: 10.1117/12.2524456

SPIE.

Event: Fifth International Symposium on Laser Interaction with Matter, 2018, Changsha, China

Dynamics character of swirling flame investigated by OH and CH2O planar laser-induced fluorescence

Hao Yan[a,b], Shaohua Zhang*[a], Xilong Yu[a,b]
[a]State Key Laboratory of High Temperature Gas Dynamics, Institute of Mechanics, Chinese Academy of Sciences, No.15 Beisihuanxi Rd., Beijing, China 100190;
[b]School of Engineering Science, University of Chinese Academy of Sciences, No.19 Yuquan Rd., Beijing, China 100049

ABSTRACT

The model combustor of aircraft engine under fuel-lean condition is characterized by planar laser-induced fluorescence (PLIF) technique. By imaging the fluorescence from OH and CH_2O simultaneously under various operation points, the transient structures of the reaction zone and preheat zone have been investigated. By the application of proper orthogonal decomposition (POD) and extended POD (EPOD) methods to the OH PLIF and CH_2O PLIF data, the main dynamics modes of the swirling flame are extracted, as well as the CH_2O PLIF signal distribution for each POD mode. The experimental results indicate that as the thermal power of the combustor increases, the time-averaged structure and dynamics modes experience notable transitions. At relatively high flow rate, local extinction occurs and unburnt fuel emerges in the external recirculation zone (ERZ).

Keywords: laser-induced fluorescence, swirling flame, OH, CH2O, proper orthogonal decomposition

1. INTRODUCTION

The swirling flame is commonly used in gas turbine combustor to hold the flame in the designated area within the combustor as well as to improve the mixing of the air and fuel in non-premixed burners. The flow is in the turbulent regime, so the flame is subject to instabilities that may be harmful to the combustor [1-3]. The situation is worsened under fuel-lean condition, of which the original purpose is to suppress the NO_x emission. Hence, investigation in the swirling flame is of great importance for evaluation of combustor designs and for validation of computational models.

The planar laser-induced fluorescence (PLIF) technique is a useful tool for flame structure visualization [4,5], and it also provides helpful data for the validation of computational models in combustion. In study of swirl-stabilized flame in the gas turbine combustor, a simultaneous dual-species PLIF system is established to measure the flame structure and data processing technique is applied to unveil the dynamic character of the flame.

The OH radicals, which exist in the flame front and the hot reaction product is commonly used as a fluorescence specie for combustion studies [5]. The CH_2O (formaldehyde) molecules are in the pre-heat zone of the flame [6]. With the imaging of the two species at the same time, the spatial distribution of the preheat zone with unburnt fuel and the reaction zone is visualized. By the application of proper orthogonal decomposition (POD) and extended POD (EPOD) methods [7,8] to the OH PLIF and CH_2O PLIF images, the main dynamics modes of the swirling flame are extracted, as well as the CH2O PLIF signal distribution for each POD mode. The experimental results indicate that as the thermal power of the combustor increases, the time-averaged structure and dynamics modes experience notable transitions. As the flame elevated, the flame exhibits stronger axial instability, while the deformation caused by precessing vortex core (PVC) is decreased. At relatively high thermal power, unburnt fuel emerges in the external recirculation zone (ERZ).

*shzh @imech.com; phone +86 10 8254 5830

Fifth International Symposium on Laser Interaction with Matter, edited by Yijun Zhao, Proc. of SPIE
Vol. 11046, 110460Q · © 2019 SPIE · CCC code: 0277-786X/19/$18 · doi: 10.1117/12.2524456

2. EXPERIMENTAL SETUP

In this study, dual-specie PLIF technique is utilized to investigate the swirling flame. The experimental set-up, sketched in Figure 1, is divided into two parts: a dual-specie PLIF system which consists of lasers, cameras, timing control, and other optics, and the swirling combustor with gas supplies.

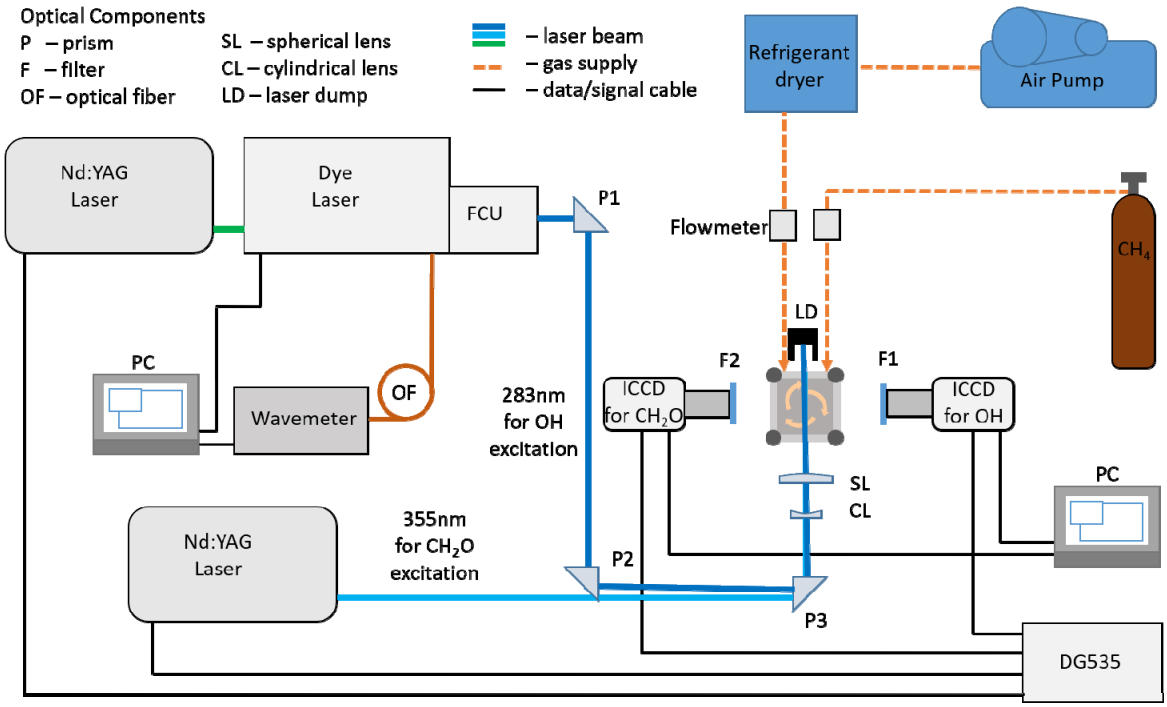

Figure 1. The experimental set-up for OH and CH_2O PLIF investigation in the swirling flame

2.1 Dual-specie PLIF system

The fluorescence species CH_2O molecules and OH radical are chosen for their distributions upstream and downstream of the flame front accordingly. In this experiment, the two fluorescent species are excited by two lasers. The OH fluorescence is excited through $Q_1(7)$ transition in the $A^2\Sigma^+ \leftarrow X^2\Pi(1,0)$ excitation band by UV laser near 283nm. The excitation laser is generated at 566nm by a tunable dye-laser (Sirah, PrecisionScan) loaded with Rhodamine 6G and up-converted to UV region through frequency doubling process in the frequency conversion unit. The dye laser is pumped by the second harmonic output of a Nd:YAG laser (Spectra-Physics, Quanta Pro) at 532nm with repetition rate of 10Hz. The maximum energy of the OH excitation laser is 20mJ/pulse. The fluorescence emission in $A^2\Sigma^+ \leftarrow X^2\Pi(0,0)$ band is captured by an ICCD (intensified charge-coupled devices) (Princeton Instrument, PI-MAX4) with bandpass filter at 307nm with FWHM of 10nm. The peak transmission of the filter is 15%. The gate width of the intensifier is set to 50ns.

The CH_2O fluorescence is excited by 355nm laser within the $A^1A_2 \leftarrow X^1A_1$ 4_0^1 band from the third harmonics output of a Nd:YAG laser (Spectra-Physics, Quanta Pro). The maximum energy of the excitation laser is 300mJ/pulse, and the pulse width is 10ns. The excited CH_2O molecules have a broad band emission from 400nm to 500nm. To maximize the fluorescence signal captured by the ICCD (Princeton Instrument, PI-MAX4), a 400 – 800nm broadband filter is placed before the ICCD lens to filter out the elastic scattering of the 355nm laser. To further suppress the interference by the excitation beam on the PLIF image, a 10ns delay is inserted between the ICCD gate and the arrival of the laser at the combustor.

As is shown in fig. x, the two excitation laser beams are close to each other. The spatial separation of the optical path before the cylindrical lens is less than 1cm. The two beams are then shaped by the cylindrical lens and spherical lens into 100-mm-high laser sheets, which enters into the combustor through the fused silica window. The two laser sheets overlap at the center of the combustor, and the spatial separation in the interrogation area is within 1mm.

2.2 Swirling combustor

The sketch of the combustor is shown in Figure 2. The air supply is connected to a plenum at the bottom of the combustor. At top of the plenum, there are two radial swirlers attached air nozzles in a concentric setup. The diameter of the inner circular nozzle is 15mm, and the outer diameters of the annual nozzle is 25mm. The fuel is injected through a narrow and non-swirling annular nozzle between the two air nozzles. The combustion chamber is surrounded by four rectangle fused silica windows that are fixed between four posts for optical access. The inner width of the square cross-section of the chamber is 90mm and the height is 110mm. On top of the combustion chamber is a plate with circular exhaust with inner diameter of 40mm.

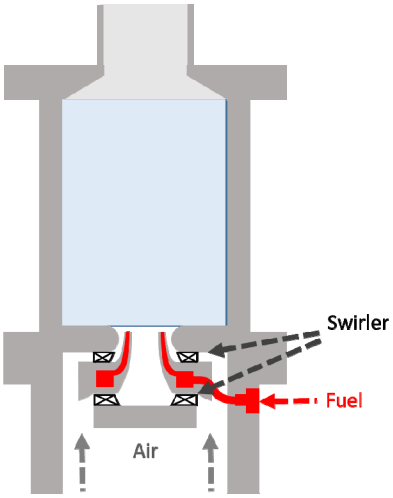

Figure 2. Schematic of the combustor.

For the operation points discussed in this article, the ambient condition of the experiment is at room temperature and atmospheric pressure. The thermal power of the fuel is ranging from 10 kW to 35kW. For all the numbered test points, listed in table 1, the air/fuel ratio is fixed at 1/0.65.

Table 1. Tested operation points.

Operation point	Power / kW	Equivalent ratio
1	10	0.65
2	15	0.65
3	20	0.65
4	25	0.65
5	30	0.65
6	35	0.65

3. RESULTS AND DISCUSSIONS

3.1 Flame structure

In this experiment, optical diagnostics were taken under various operation points listed in Table 1. The flame structure was investigated by simultaneous OH and CH_2O PLIF measurements. The transient single shot OH PLIF measurements are illustrated in Figure 3. At low flow rate, the combustion reactions take place mainly near the central axis of the combustor. The reaction zone expand to the downstream direction as the flow rate increases. In the OH PLIF images, the LIF signal emerges at the lower corners, indicating that the flow is recirculating at the outer part of the combustor (external recirculation zone, ERZ). The simultaneous OH and CH_2O PLIF is shown in Figure 4, where the red channel represents the OH PLIF signal and green channel the CH_2O PLIF signal. The OH and CH_2O species do not overlap in the flame. Compared with unconfronted swirl flame [9], the CH2O layer is much thicker. The widening in preheat zone is caused by the formation of ERZ, so fresh fuel is heated by the mixing with hot combustion product.

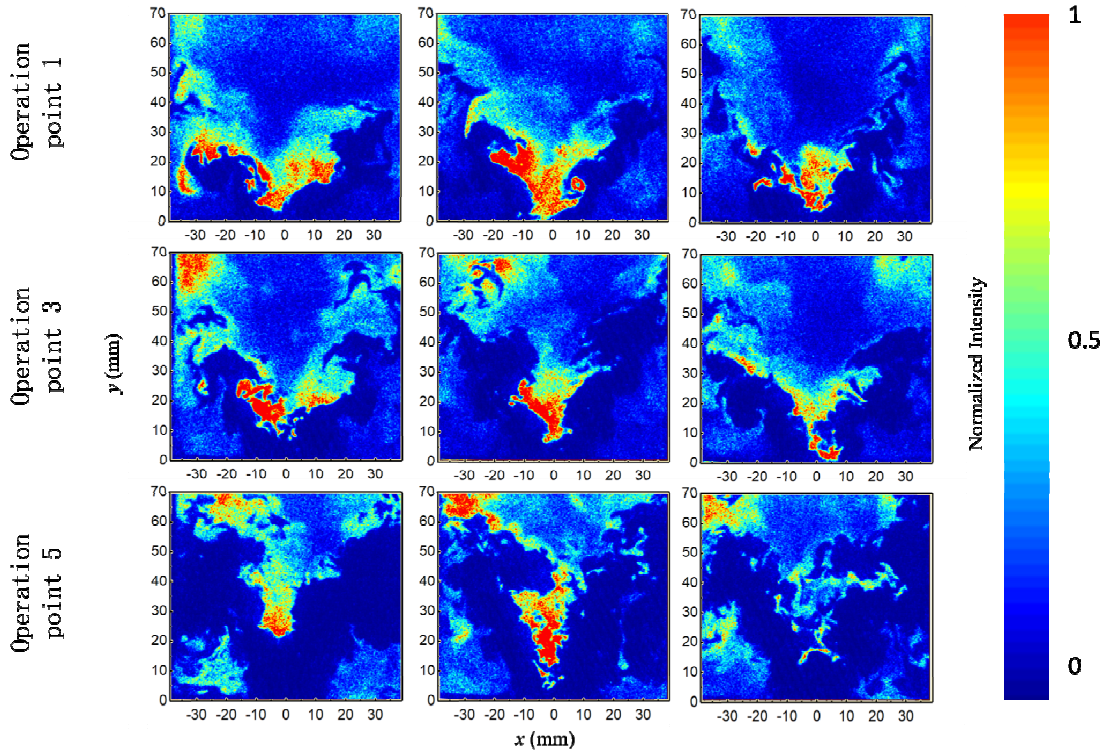

Figure 3. Single-shot OH PLIF images under different operation points.

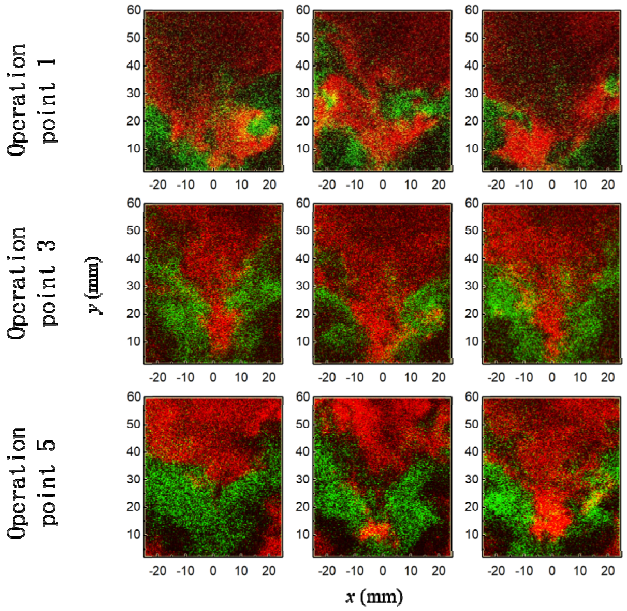

Figure 4. Simultaneous OH (red) and CH_2O (green) PLIF images un-der different operation points.

The time-averaged OH and CH_2O PLIF images for various operation points are shown in Figure 5 and Figure 6. At low flow rate, the OH PLIF image is V-shaped, as the signal at the center of the combustor is relatively weak. As the flow rate increases, the distribution of OH PLIF signal is raised, forming a triangular area, and the signal at the lower corner (ERZ) of the combustor becomes stronger. Meanwhile, the distribution of CH_2O signal remains V-shaped under all tested operation points. Although OH and CH_2O do not coexist in the flame, the PVC caused flame root to oscillate in the radial direction. As a result, the time-averaged OH and CH_2O distributions overlap at low thermal power.

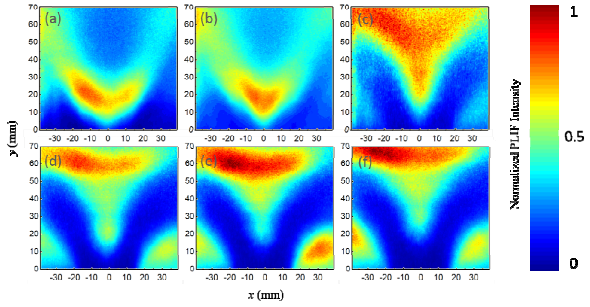

Figure 5. Averaged OH PLIF images under different operation points. (a) – (f) for operation point 1 – 6 accordingly.

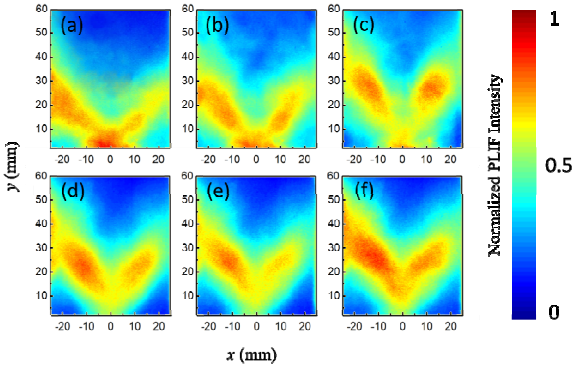

Figure 6. Averaged CH_2O PLIF images under different operation points. (a) – (f) for operation point 1 – 6 accordingly.

3.2 Dynamic modes of the flame

In this study, POD is applied to the measured data to investigate the dynamic modes of the flame. The POD and EPOD and snapshot methods have been well explained in previous studies [8,10].

For PLIF data, the POD modes are extracted from 500 OH PLIF samples for each tested operation point. EPOD is applied to the CH_2O data. The CH_2O PLIF images are treated as supplementary data to the OH PLIF measurements. Before the decomposition, a 2D FFT filter is applied to all samples to suppress the interference from the readout noise and a 3x3 median filter to reduce the random noise. Shown in Figure 7, the energy spectrum of POD modes for operation point 1 indicates that the energy of modes converges rapidly on the mode number.

The 0th modes of OH PLIF POD and CH_2O PLIF EPOD are the averaged signal shown in Figure 5 and Figure 6. The first 6 POD modes for operation point 1 are shown in Figure 8 in pseudo-color. The mode 1 represents the extinction of the flame root since the flame is approaching blow-out under the lean fuel condition. Both of the mode 2 and 3 exhibits anti-symmetry. The mode 2 indicates the strength of the PLIF signal alters between left and right. The mode 3 indicates the twisting of the flame. The two modes are coupled together, representing the twisting of the flame caused by PVC. The mode 4 and 6 are symmetric, representing that the reaction zone is oscillating between the central and outer part of the combustor. The EPOD modes of CH_2O PLIF exhibit similarity to the POD modes except that the sign of the values is opposite. It is consistent with the observation that OH and CH_2O do not overlap.

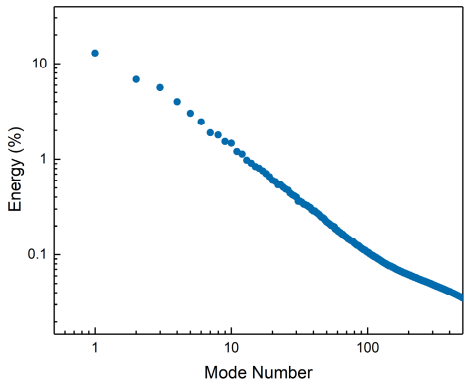

Figure 7. Energy distribution over OH PLIF POD modes under operation point 1.

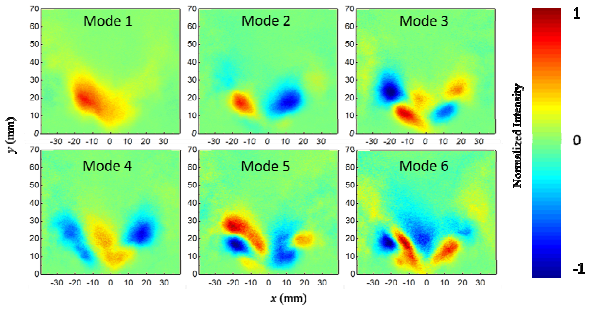

Figure 8. POD modes of OH PLIF under operation point 1.

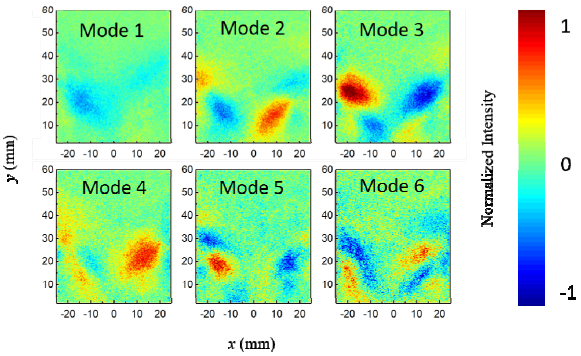

Figure 9. Extended POD modes of CH_2O PLIF under operation point 1.

The OH* CL at operation point 1 is recorded by highspeed camera to support the dynamic character analysis. The POD modes of the CL measurement are shown in Figure 10, as well as the evolution of the coefficient of each mode for a short period of time in Figure 11. The mode 1 and 2 representing axial oscillation of the flame evolves at the same frequency with a phase difference of $\pi/2$. The same feature can be found in mode 3 and 4, which represents the PVC of the flame. The evolution the two types of oscillation with phase interval of $\pi/2$ is illustrated in Figure 12. A Fourier analysis of the mode coefficients indicates the frequencies of the radial and PVC oscillation are 310 and 530Hz accordingly.

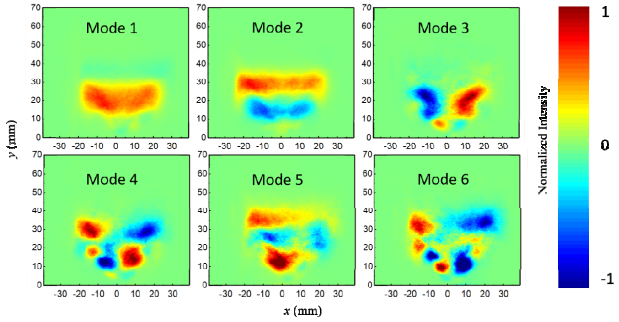

Figure 10. POD modes of OH* CL under operation point 1.

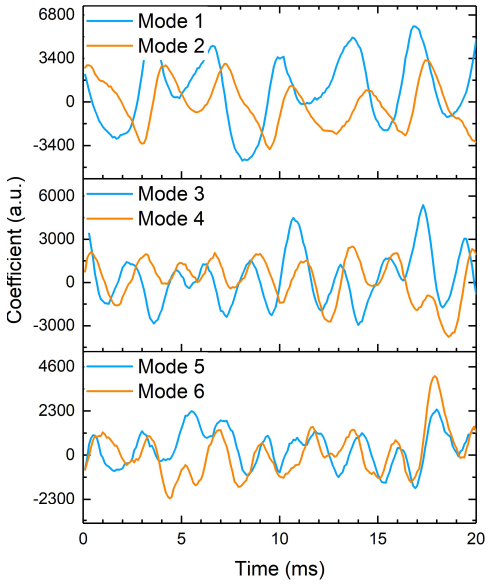

Figure 11. The evolution of the coefficient of POD modes of OH* CL under operation point 1.

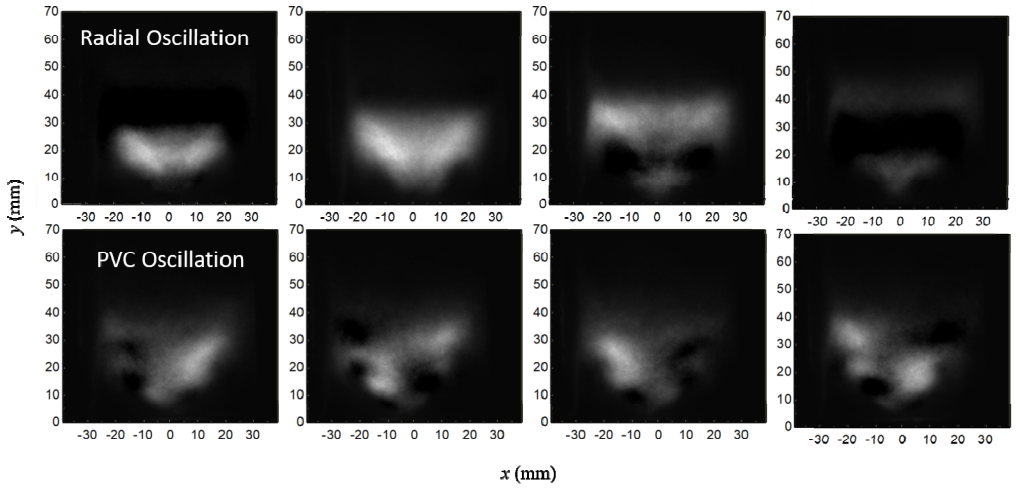

Figure 12. The evolution of the radial oscillation and PVC oscillation with 90° phase separation.

The POD modes of OH PLIF at operation point 3 and 5 are shown in Figure 13 and Figure 14 accordingly. The shapes of the modes change significantly as the thermal power increases. It worth noting that at operation point 5, the POD modes are no longer symmetric or antisymmetric. The mode 2 represents the variation of the OH PLIF signal at the lower right corner of the combustor, such variation at the lower left corner, however, is not significant as it is not captured in the low order POD modes. This indicates that the flow may be susceptible to the asymmetric in the burner at high flow rate. The EPOD modes of CH_2O PLIF at operation point 3 and 5 are shown in Figure 15 and Figure 16 accordingly. The correlation between the POD and EPOD modes is still strong under high flow rate when the symmetric properties of the POD modes disappears. At operation point 5, the mode 2 of EPOD indicates that the variation of the PLIF signal of the two species are negatively correlated. This indicates local extinction occur as the unburnt mixture with CH_2O but no OH radical emerges in that area.

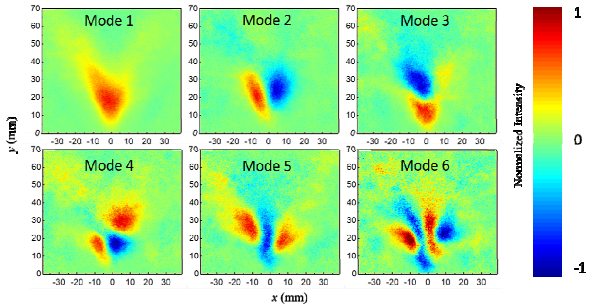

Figure 13. POD modes of OH PLIF under operation point 3

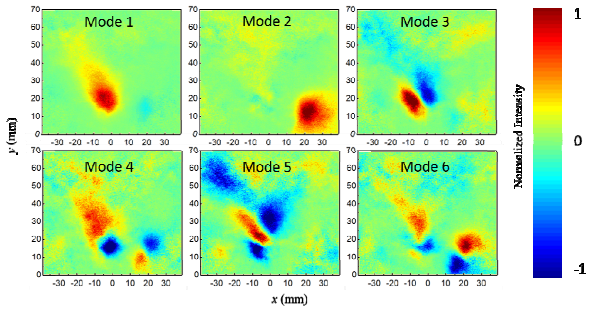

Figure 14. POD modes of OH PLIF under operation point 5

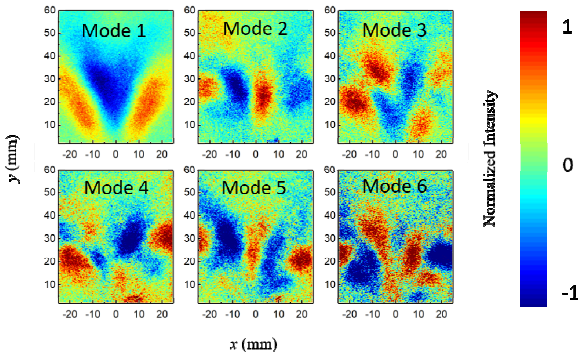

Figure 15. Extended POD modes of CH_2O PLIF under operation point 3

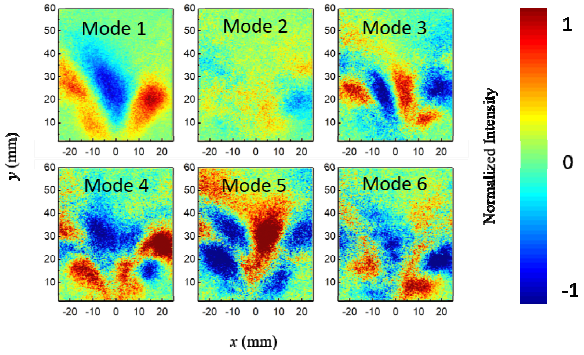

Figure 18. Extended POD modes of CH_2O PLIF under operation point 5.

4. CONCLUSION

The dual-specie PLIF technique for swirling flame is discussed in this paper. The results show that the simultaneous OH and CH_2O PLIF measurement is capable of capturing the transient structure of the preheat zone and reaction zone of the swirling flame. The flame exhibits turbulent features. By applying the POD analysis to the data, the dynamic mode of flame oscillation caused by PVC is recognized. As the flow rate increases, the time-averaged structure as well as the POD mode change dramatically. The EPOD analysis shows that the CH_2O distribution is strongly correlated to the POD mode of OH distribution under all the tested operation points. By correlating the dynamic modes OH and CH_2O PLIF measurement, it is obvious to determine where unburnt fuel is likely to emerge and which dynamic mode it is related. It is possible to identify if the combustion is complete at high flow rate.

ACKNOWLEDGEMENTS

This work was sponsored by the National Natural Science Foundation of China (Grant Nos. 11672359).

REFERENCES

[1] Syred, N., "A review of oscillation mechanisms and the role of the precessing vortex core (PVC) in swirl combustion systems," Prog. Energy Combust. Sci. Papers 32(2), 93–161 (2006).

[2] Renard, P. H., Thevenin, D., Rolon, J. C. and Candel, S., "Dynamics of flame/vortex interactions," Prog. Energy Combust. Sci. Papers 26(3), 225–282 (2000).
[3] Candel, S., Durox, D., Schuller, T., Bourgouin, J. and Moeck, J. P., "Dynamics of Swirling Flames," Annu. Rev. Fluid Mech. Papers 46(1), 147-161 (2013).
[4] Crosley, D. R. and Smith, G. P., "Laser-induced fluorescence spectroscopy for combustion diagnostics, " Opt. Eng. Papers 22(5), 545-553 (1983).
[5] Hanson, R. K., Seitzman, J. M. and Paul, P. H., "Planar laser-fluorescence imaging of combustion gases," Appl. Phys. B Papers 50(6), 441-454 (1990).
[6] Mohlmann, G. R., "Formaldehyde Detection in Air by Laser-Induced Fluorescence, " Appl. Spectrosc. Papers 39(1), 98-101 (1985).
[7] Sirovich, L., "Turbulence and the dynamics of coherent structures part I: coherent structures, " Quart. Appl. Math. Papers 45(3), 561-571 (1987).
[8] Boree, J., "Extended proper orthogonal decomposition: a tool to analyse correlated events in turbulent flows," Exp. Fluids Papers 35(2), 188–192 (2003).
[9] Zhou, B., Li, Q., He, Y., Peterson, P., Li, Z., Alden, M. and Bai, X., "Visualization of multi-regime turbulent combustion in swirl-stabilized lean premixed flames," Combust. Flame Papers 162(7), 2954–2958(2015).
[10] Stohr, M., Sadanandan, R. and Meier, W.. "Phase-resolved characterization of vortex–flame interaction in a turbulent swirl flame," Exp. Fluids Papers 51(4), 1153–1167 (2011).